pH Dependence and Structural Interpretation of the Reactions of *Coprinus cinereus* Peroxidase with Hydrogen Peroxide, Ferulic Acid, and 2,2′-Azinobis(3-ethylbenzthiazoline-6-sulfonic acid)†

A. Katrine Abelskov,‡ Andrew T. Smith,§ Christine Bruun Rasmussen,‡ H. Brian Dunford,|| and Karen G. Welinder*,‡

Department of Protein Chemistry, University of Copenhagen, Øster Farimagsgade 2A, DK-1353 Copenhagen K, Denmark, School of Biological Sciences, University of Sussex, Brighton, East Sussex BN1 9QG, U.K., and Department of Chemistry, University of Alberta, Edmonton, Alberta, Canada T6G 2G2

Received February 19, 1997; Revised Manuscript Received May 20, 1997⊗

ABSTRACT: Steady-state and transient-state analysis of *Coprinus cinereus* peroxidase, CIP (identical to *Arthromyces ramosus* peroxidase), was used to characterize the kinetics of the three fundamental steps in heme peroxidase catalysis: compound I (cpd I) formation, cpd I reduction, and compound II (cpd II) reduction. The rate constant k_1 for cpd I formation determined by transient-state analysis is $(9.9 \pm 0.6) \times 10^6$ M^{-1} s^{-1}. The k_1 determined by steady-state analysis is $(8.8 \pm 0.6) \times 10^6$ M^{-1} s^{-1} in the presence of ferulic acid and $(6.7 \pm 0.2) \times 10^6$ M^{-1} s^{-1} in the presence of ABTS. The value of k_1 is constant from pH 6 to 11. However, at low pH the value of k_1 decreases, corresponding to titration of an enzyme group with a pK_a of 5.0. Titration of this group is also detected from cyanide-binding kinetics. Furthermore, titration of this group is linked with marked spectroscopic changes unique to CIP. We ascribe these changes to protonation of proximal His183. A very low pK_a is proposed for distal His55 in the resting state of CIP. The rate constants, k_2 for cpd I and k_3 for cpd II reduction, are very large for both ferulic acid and 2,2′-azinobis(3-ethylbenzthiazoline-6-sulfonic acid) (ABTS). For ferulic acid, transient-state kinetic analysis shows that the values of k_2 and k_3 are identical at pH 5−6, and the ratio k_2/k_3 increases to 10 at pH 10. The similar magnitude of k_2 and k_3 is unusual for a peroxidase. Both k_2 and k_3 decrease with increasing pH, and both are influenced by two ionizations: one with a pK_a value near 7, assumed to reflect the protonation of His55; and the other with pK_a of 9.0 ± 0.7 for k_2 and 8.8 ± 0.4 for k_3, perhaps reflecting the phenol-linked deprotonation of ferulic acid. Steady-state analysis at pH 7.0 gave $k_2k_3/(k_2 + k_3) = (2.2 \pm 0.1) \times 10^7$ M^{-1} s^{-1} for ferulic acid, and $(2.0 \pm 0.7) \times 10^7$ M^{-1} s^{-1} for ABTS and revealed a unimolecular step with $k_u = 1500$ s^{-1}, ascribed to slow ABTS radical product release. From transient-state results at pH 7, the values of k_2 and k_3 were found to be identical also for ABTS. A mechanism for cpd I and II reduction involving distal histidine and arginine is proposed.

Peroxidase is an enzyme that has been used in diverse practical applications. It is widely used in analytical chemistry in coupled enzyme assays (blood sugar, cholesterol), immunochemistry, and in biosensor construction. It can oxidize colored substrates rapidly, and therefore has great potential in the textile, paper and pulp bleaching industries. In addition, peroxidases play important roles in food processing and storage. Peroxidase (E) consumes peroxide and oxidizes a broad range of organic molecules (AH) to radicals ($A^\bullet$) in two sequential one-electron steps via the intermediates cpd I and II:[1]

$$E + H_2O_2 \xrightarrow{k_1} \text{cpd I} + H_2O \quad (1)$$

$$\text{cpd I} + AH \xrightarrow{k_2} \text{cpd II} + A^\bullet \quad (2)$$

$$\text{cpd II} + AH \xrightarrow{k_3} E + A^\bullet + H_2O \quad (3)$$

The radicals can then disproportionate or initiate a variety of nonenzymatic reactions including degradation and polymerization processes.

Evolutionarily related heme-containing peroxidases are found in bacteria and organelles of prokaryotic origin (class I), fungi (class II), and plants (class III) (*1*). Recently a fungal peroxidase from *Coprinus cinereus* (identical to *Arthromyces ramosus* peroxidase) has attained much attention due to the ease of production, high specific activity, and broad substrate specificity similar to that of the classical horseradish peroxidase. Shinmen et al. (*2*, *3*) were the first to isolate and characterize this novel peroxidase from the medium of the fungal mycelia. The taxonomic characteristics of the fungal strain were similar to those of the genus *Coprinus* (*Basidiomycota*, *Basidiomycetes*, *Agaricales*), but

† This work was supported by the EU Human Capital and Mobility Program (ERBCHRX-CT92-0012 to K.G.W. and A.T.S.), The Danish Research Academy (S940173), and a Novo Nordisk A/S scholarship to A.K.A.

* Author to whom correspondence should be addressed: Tel + 45 35322077; Fax +45 35322075; E-mail welinder@biobase.dk.

‡ University of Copenhagen.

§ University of Sussex.

|| University of Alberta.

⊗ Abstract published in *Advance ACS Abstracts,* July 15, 1997.

[1] Abbreviations: ABTS, 2,2′-azinobis(3-ethylbenzthiazoline-6-sulfonic acid); AMS, ammonium sulfate; ARP, *Arthromyces ramosus* peroxidase; CCP, yeast cytochrome *c* peroxidase; CIP, *Coprinus cinerius* peroxidase; cpd I and cpd II, compound I and II; HRP C, horseradish peroxidase isoenzyme C.

S0006-2960(97)00387-5 CCC: $14.00

the perfect stage of the life cycle was not found, and therefore the fungus was classified as a fungi imperfecti and given the name *Arthromyces ramosus*. Morita et al. (*4*) described the molecular and biophysical properties of a similar peroxidase from *Coprinus cinereus*. In this laboratory we found that *Coprinus cinereus* peroxidase (CIP), commercial samples of *Coprinus macrorhizus* peroxidase, and *Arthromyces ramosus* peroxidase (ARP) were identical in size, shape, isoelectric point, and amino acid composition. CIP and ARP also showed immunochemical identity, and gave the same reaction rates in steady-state experiments using guaiacol at pH 6.0−10.0 or iodide at pH 3.3−7.0 (*5*). Recently, the crystal structures of CIP (*6*) and of ARP (*7*, *8*) were determined and found to be indistinguishable. Protein and cDNA sequencing of CIP in combination identified a 20 residue signal peptide followed by a 343 residue mature protein blocked with pyroglutamate (*9*; EMBL data bank X69457). These data and genomic sequencing (*10*; EMBL data bank X70789) suggested the presence of one CIP gene only, which is split by 14 introns. Two allelic forms were found, which were 96% identical at the cDNA level and differ at only one amino acid residue, Val-199-Ile. The data were recently confirmed for ARP (*11*), except for one additional glycine residue near the N-terminus of the mature protein. Commercial ARP from Sigma (lot 42HO959) did not contain the additional glycine residue, however (Welinder, unpublished result). The divergence appears to have no functional implications but will offset all active-site residue numbers by one when comparing CIP and ARP. In this paper we use CIP residue numbers 1−343 for the mature protein. CIP (*12*) and many active-site, substrate interaction site, and glycosylation mutants of CIP (*13*) have been expressed in *Aspergillus oryzae* in high yields. The natural fungal CIP and recombinant CIP were shown by protein chemical analysis (*14*), proton NMR spectroscopy (*15*), and resonance Raman and electronic absorption spectroscopy (*16*) to be identical in all respects. Indeed, the crystallographic studies of CIP were carried out on the recombinant protein (*6*). The results of structure−function studies obtained using CIP purified from *Coprinus*, recombinant CIP, or ARP should be equivalent.

CIP shows enzymatic properties similar to those of horseradish peroxidase (HRP C) and yet very different from those of fungal lignin and Mn peroxidases when assayed at pH 7 and 5 (*2*−*4*, *17*), despite the fact that CIP is only 18% identical in amino acid sequence to HRP C but 40−45% identical to these fungal peroxidases (*9*). The crystal structures of CIP and lignin peroxidase (*7*) are highly similar, exhibiting 1.25 Å rms difference in C_α atoms. The functional similarity to HRP C also extended to a broad and rather high pH optimum for phenolic compounds (*3*, *5*). In chemiluminiscent oxidation of luminol, CIP was a 100-fold more efficient catalyst than HRP C (*18*, *19*).

It is important to compare and contrast the properties of model members of each of the three classes of peroxidases in which a common heme center and active-site residues are displayed on a common fold yet with an extensive variability in amino acid sequence. The detailed structures derived by X-ray crystallography and NMR and resonance Raman spectroscopy and the mechanism of cpd I formation have been particularly well studied in yeast cytochrome *c* peroxidase (CCP), a class I peroxidase, together with a large number of site-directed mutants (reviewed in refs *20* and *21*). The situation is similar for HRP C, the prototypic class III peroxidase, excepting that structural reference can be made only to the similar peanut peroxidase (*22*) at present. Kinetics of oxidation of small substrates by HRP C has been reviewed by Dunford (*23*). Among the class II peroxidases the atypical lignin and Mn peroxidases are best known. CIP/ARP, however, appears to provide a more general model peroxidase of the fungal class (*17*).

We present a detailed kinetic characterization of CIP over the pH range 3.8−10.5. A mechanism for the reduction of CIP cpd I and cpd II is proposed. Furthermore, the kinetic properties of CIP are discussed in relation to the structural information available for CIP and the comprehensive knowledge of structure−function relationships for CCP and HRP C. These CIP wild-type studies will, in addition, provide a frame of reference for studies in progress on heme active-site mutants of CIP and mutants at the site of reducing substrate interaction.

MATERIALS AND METHODS

Enzyme Preparation. Recombinant *Coprinus cinereus* peroxidase (CIP) expressed in *A. oryzae* has been used throughout this study. The material was produced according to Dalbøge et al. (*12*) and purified and characterized as described previously (*14*). It did not contain any des-pyrrolidoneglutamyl-1 variant and was highly homogeneous with respect to the size of the one N-linked and the two O-linked glycans, despite the fact that these naturally occurring variations do not appear to have any influence on CIP kinetics (*5*). Furthermore, a low-spin form of CIP was not present. This form might appear to various extents in different fermentation batches and must be removed by ion-exchange chromatography, as NMR experiments have shown that it is not in equilibrium with other spin forms and must be considered an artifact (*24*). The purified protein was stored as an ammonium sulfate (AMS) precipitate. Enzyme samples, RZ > 2.3, used for steady-state experiments were prepared by centrifugation and the precipitate was dissolved in 10 mM $CaCl_2$. The RZ value increased to greater than 2.6 after dialysis against 1 mM $CaCl_2$. The Soret band maximum and intensity was shown to be sensitive to the composition of the peroxidase solution, and it has recently been shown that ammonia binds to the enzyme, giving a low-spin CIP complex (*8*). The ϵ_{280} was 35 mM^{-1} cm^{-1} determined by amino acid analysis (K. G. Welinder, unpublished work). Due to the low concentrations of enzyme used in steady-state experiments, the residual AMS was neglected. For transient-state experiments the AMS pellet was dissolved in buffer and then desalted by either gel filtration or dialysis against buffer. The concentration of CIP was determined using ϵ_{405} = 109 mM^{-1} cm^{-1} (*25*).

Substrates. H_2O_2 was stored as 10−50 mM stock solutions. The concentration was determined and checked daily using an extinction coefficient of 43.6 M^{-1} cm^{-1} at 240 nm (*26*). 2,2′-Azinobis(3-ethylbenzthiazoline-6-sulfonic acid) (ABTS) and ferulic acid were obtained from Sigma. Fresh solutions were made every day. The concentration of ABTS was determined using ϵ_{340} = 36.6 mM^{-1} cm^{-1} (*27*). The concentration of ferulic acid was determined using ϵ_{310} = 16.0 mM^{-1} cm^{-1} (L. Østergaard, personal communication). All substrate solutions were stored cold and in the dark, until immediately before use. Extinction coefficients were determined as described by Rasmussen et al. (*28*).

Buffers. For steady-state measurements pH 4−6, 10 mM citrate buffer plus 1 mM $CaCl_2$ was used; at pH 7, 10 mM phosphate buffer was used; and at pH 8.5−10, 20 mM borate plus 10 mM phosphate buffer was used. The ionic strength was adjusted to 0.1 with potassium sulfate. The buffers used for transient-state analyses with ferulic acid were 10 mM borate at pH 10 and 9, 10 mM phosphate at pH 7, 15 mM phosphate at pH 6, and 5 mM citrate at pH 5. By varying the buffer concentration, the ionic strength was kept constant at 0.015 M except at pH 10 and 9, where the ionic strength was 0.01 M.

Steady-State Experiments. Kinetic experiments were performed using a Hewlett-Packard 8452 diode-array spectrophotometer, equipped with a stopped-flow SFA-12 rapid kinetics accessory and an OPT-12P pneumatic drive, both from Hi-Tech Scientific. The temperature was held constant at 25 °C by a Hewlett-Packard 89090A Peltier temperature controller. The stopped-flow device has a dead time of 0.1 s and a total reaction volume of approximately 400 μL. The enzyme solution was placed in one syringe, and H_2O_2 and reducing substrate were placed in the other. Rates were determined as the slope of the initial change in absorbance. Formation of ABTS radical product was measured using $\epsilon_{414} = 36.6\ mM^{-1}\ cm^{-1}$, which was found to be similar and stable at pH 4, 7, and 10 (data not shown). In ferulic acid experiments the consumption of substrate was measured at 310 nm using $\Delta\epsilon = 8.68\ mM^{-1}\ cm^{-1}$ (L. Østergaard, personal communication). Initial rates were measured over 10 s. The concentration of the reducing substrates was kept constant and the concentration of H_2O_2 was varied in each experiment. Final concentrations of 3−10 nM CIP gave rates that could be accurately measured. An enzyme blank was measured to correct for autooxidation, when necessary. Rate equations are derived in the appendix.

Transient-State Experiments. The reaction of CIP with H_2O_2 was measured as a decrease in absorbance at 405 nm on a Union Giken RA-601 rapid reaction analyzer. The final concentration of enzyme was 1 μM, and the final concentration of H_2O_2 was varied between 10 and 30 μM to obtain pseudo-first-order conditions. The bimolecular reactions between cpd I or cpd II and reducing substrates were measured at 25.0 ± 0.2 °C using the SX-18MV stopped-flow instrument from Applied Photophysics. The kinetics at pH 5.0 and 6.0 was analyzed by pH-jump in order to obtain reproducible results, preparing the enzyme in water adjusted to pH 7.0 with phosphate buffer. Substrate solutions were made up in buffer of twice the final concentration. The pH was checked after mixing. Determination of k_2 and k_3 at pH 10.5 also required pH-jump experiments due to insufficient stability of cpd I.

Both steady-state and transient-state rates were determined as the mean of at least five experiments with a deviation of no more than 10% from the mean.

RESULTS

Steady-State Kinetics with ABTS and Ferulic Acid. Steady-state experiments were performed at pH 7.0. Families of rectangular hyperbolae were obtained by varying H_2O_2 concentrations up to 1 mM, at six fixed concentrations of ABTS ranging from 10 to 500 μM (Figure 1A), and for five fixed concentrations of ferulic acid 10−100 μM (Figure 1B). It was not possible to measure rates of ferulic acid oxidation at concentrations higher than 100 μM due to its high intrinsic absorbance. The initial rate $v/2E_0$ was plotted versus H_2O_2 concentration (Figure 1), and the parameters *A* and *B* were determined according to eq A13 (Appendix). Plots of *A* versus *B* will give straight lines with a slope of k_1 (Figure 2), the bimolecular rate constant for cpd I formation, irrespective of whether the classic peroxidase mechanism, eqs 1−3 (*23, 28*), or the modified mechanism (*29*), eqs A1−A3b (Appendix), is obeyed. The value of k_1 determined with ABTS as substrate was $(6.7 \pm 0.2) \times 10^6\ M^{-1}\ s^{-1}$, and with ferulic acid, $(8.8 \pm 0.6) \times 10^6\ M^{-1}\ s^{-1}$.

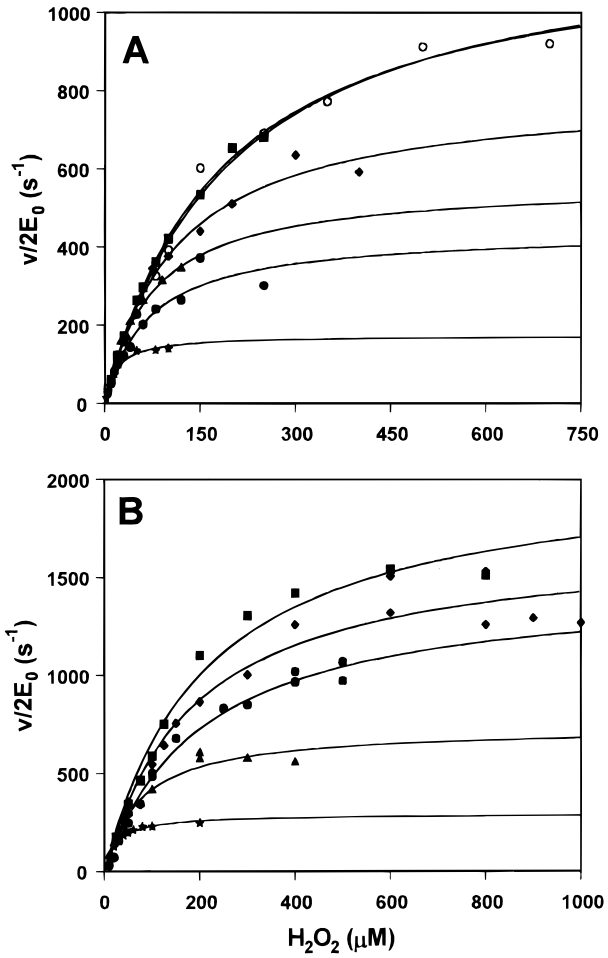

FIGURE 1: Steady-state initial rates are plotted versus H_2O_2 concentration, (A) using ABTS at 10 (★), 25 (●), 50 (▲), 75 (◆), 200 (■), and 500 μM (○) concentration or (B) ferulic acid at 10 (★), 25 (▲), 50 (●), 75 (◆), and 100 μM (■) concentration. The curves can be fitted by two parameters *A* and *B* determined from eq A13. Experiments were performed at 25 °C in 10 mM phosphate buffer, ionic strength adjusted to 0.1 M with potassium sulfate, pH 7.0.

Plots of parameter *A* versus concentration of reducing substrate give a straight line with slope k_3 for most peroxidase reactions (eq A16b), assuming that $k_2 \gg k_3$. The k_3 values obtained in this way for ABTS and ferulic acid (see below) were so high, however, that the assumption appeared unlikely to hold for CIP. Therefore, the general expression for the slope, $k_2k_3/(k_2 + k_3)$ according to eq A16a, was used. Figure 3 shows that ferulic acid gives a straight line with the slope $k_2k_3/(k_2 + k_3) = (2.2 \pm 0.1) \times 10^7\ M^{-1}\ s^{-1}$, whereas the ABTS data do not give a straight line. The ABTS data can be fitted to a rectangular hyperbola according to eq A14, derived assuming a mechanism including one or more unimolecular steps such as product release (*29*). Fitting the

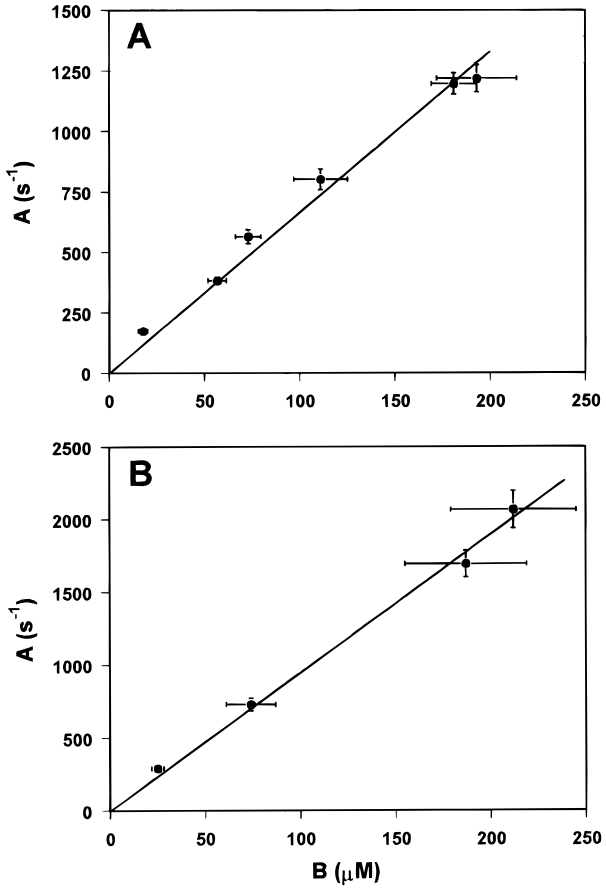

FIGURE 2: Steady-state parameter *A* plotted versus parameter *B* (eq A13) derived from the data in Figure 1. The slope of the straight line gives the rate constant k_1 (eq A15) for the reaction of CIP and H_2O_2. (A) For the ABTS reaction, k_1 is $(6.7 \pm 0.2) \times 10^6$ $M^{-1}s^{-1}$. (B) For the ferulic acid reaction, k_1 is $(8.8 \pm 0.6) \times 10^6$ M^{-1} s^{-1}.

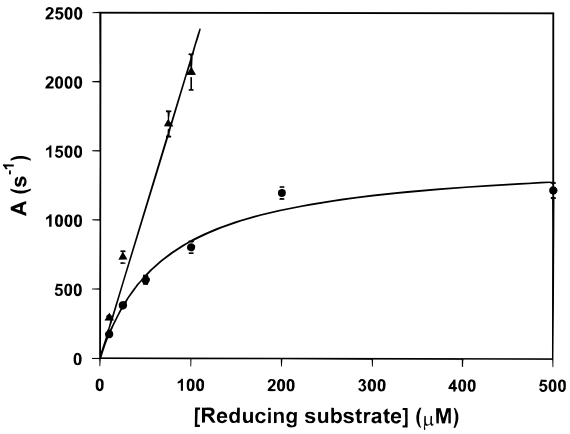

FIGURE 3: Parameter *A* plotted versus concentration of ABTS (●), and ferulic acid (▲). The rate constant k_u for the dissociation of product, eq A3b, and $k_2k_3/(k_2 + k_3)$ for the reactions with ABTS were determined by fitting to eq A14, giving $(1.5 \pm 0.1) \times 10^3$ s^{-1} and $(2.0 \pm 0.7) \times 10^7$ $M^{-1}s^{-1}$, respectively. For the reactions with ferulic acid $k_2k_3/(k_2 + k_3)$ was determined by fitting to eq A16a giving $(2.2 \pm 0.1) \times 10^7$ M^{-1} s^{-1}.

ABTS data gives the rate constants $k_u = (1.5 \pm 0.1) \times 10^3$ s^{-1} and $k_2k_3/(k_2 + k_3) = (2.0 \pm 0.7) \times 10^7$ M^{-1} s^{-1}. Consequently both ABTS and ferulic acid are very good substrates for CIP.

The parameters *A* and *B* were determined over the pH range 3.8−10.0 using 50 μM ABTS. In both the classic (*28*) and the modified peroxidase mechanism (Appendix) the rate of cpd I formation, k_1, can be determined as *A*/*B* according to eq A15. In Figure 4, k_1 is plotted as a function of pH. As can be seen, k_1 is constant from pH 6 to 10, and decreases below pH 6 with a pK_a of 5.0 (determined by fitting to $k_1 = [k_{1,a}10^{(pK_a-pH)} + k_{1,b}]/[1 + 10^{(pK_a-pH)}]$, where $k_{1,a}$ and $k_{1,b}$ are the pH-independent k_1 values of the acid and basic forms, respectively).

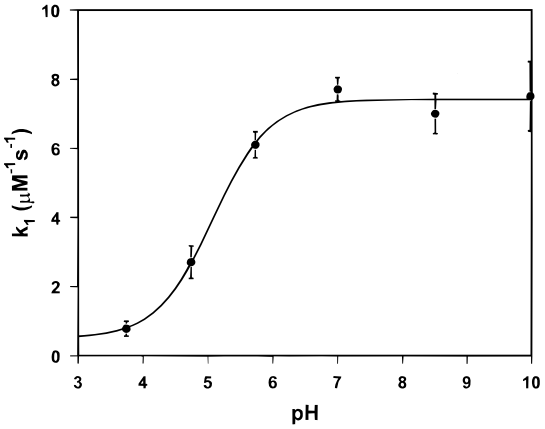

FIGURE 4: pH dependence of the rate constant k_1 for cpd I formation of CIP determined by steady-state kinetics. The parameters *A* and *B* were determined at different pH values with 50 μM ABTS as reducing substrate. k_1 was determined as *A*/*B* according to eq A15.

Transient-State Determination of k_1. The rate constant k_1 for the reaction between CIP and H_2O_2 was determined at pH 7.0. The k_{obs} values obtained by fitting the decrease in the Soret maximum to a single exponential decay were plotted against H_2O_2 concentration according to $k_{obs} = k_1[H_2O_2]$ (data not shown). A k_1 value of $(9.9 \pm 0.6) \times 10^6$ M^{-1} s^{-1} was determined, which is in very good agreement with the published value (*30*) and with the values determined from the steady-state experiments. Therefore, no further determinations of k_1 were made.

Transient-State Determination of k_2 and k_3. The isosbestic points between the different enzyme species in the peroxidase cycle at pH 7−10 have been listed by Andersen et al. (*30*). The situation is different below pH 7, however, as initial transient-state analysis of the reduction of cpd I recorded at 400 nm at pH 6.0 appeared to show only a single phase. In order to investigate this phenomenon more thoroughly, stopped-flow rapid-scan spectra were recorded (Figure 5). The simplest model consistent with the data was the standard peroxidase cycle, and the concentration of intermediates was therefore calculated after single-value deconvolution analysis using the global analysis software of the Applied Photophysics instrument. The ratio of the values of k_2 and k_3 was 1.5, explaining why cpd II was not readily detectable. The spectra of resting state CIP and the reaction intermediates cpd I and cpd II were calculated, and their isosbestic points were applied for the kinetic measurements between pH 5 and 6.

The bimolecular rate constants for the reduction of cpd I to cpd II, k_2, and for cpd II reduction, k_3, were determined with ferulic acid as reductant. Cpd I was prepared from CIP and H_2O_2 (1:2) and used within 15 min. Cpd I was reacted with ferulic acid under pseudo-first-order conditions, and the increase in absorbance at the isosbestic point between cpd II and resting state CIP, at 419 nm for pH 5−6, and at 414 nm for pH 7.0−10.5, was measured giving k_2 (Table 1). Due to the very large k_{obs} values obtained at pH 7.0−9.5, k_2 could have been underestimated at these pH values. Some of the

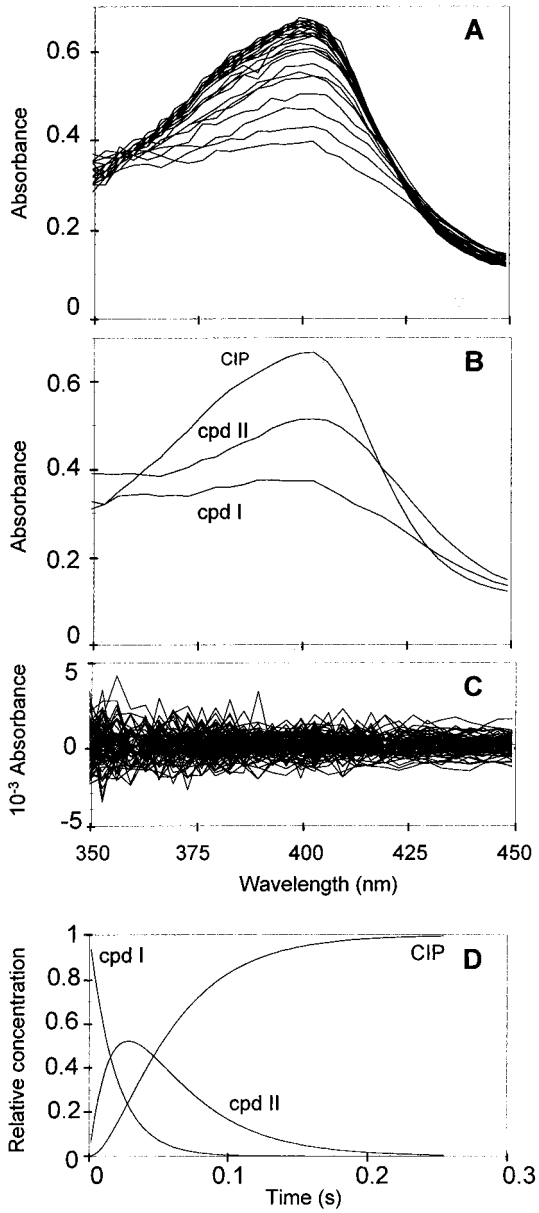

FIGURE 5: Spectra of resting state CIP, cpd I, and cpd II at pH 6.0. (A) Rapid-scan diode-array spectra of the reaction between cpd I and ferulic acid (8 μM) in 15 mM phosphate buffer, pH 6.0, recorded for 0.25 s. The absorbance increases from cpd I via cpd II to resting state CIP. The lack of a single isosbestic point implies the presence of cpd II and the data were therefore fitted to the mechanism cpd I → cpd II → resting state. (B) The calculated spectra of cpd I, cpd II, and resting state CIP. (C) Residual absorbance between the calculated and experimental spectra. (D) The calculated relative concentrations of cpd I, cpd II, and resting state during the reaction.

k_2 determinations showed small but significant positive intercepts. Positive intercepts were not obtained using vanillic acid as substrate (Othman et al., manuscript in preparation) nor in the k_3 determinations below.

Two methods, which gave identical numerical values, were used for determining k_3 (Table 1). (i) Cpd II was prepared from cpd I and $K_4Fe(CN)_6$ (1:0.9), and k_{obs} for the reduction of cpd II with ferulic acid was measured, (a) from the decrease in absorbance at the isosbestic point between resting state enzyme and cpd I, 430 nm at pH 5−6 and 426 nm at pH 7−10. Alternatively (b), the increase in absorbance at the isosbestic point between cpd I and cpd II at 395 nm was followed at pH 5−6. (ii) In turnover experiments cpd I reacted directly with ferulic acid, and the reaction was followed at the isosbestic point for resting state enzyme and cpd I. Determinations of k_3 at pH 9.0 using both methods are compared in Figure 6. The slopes, and hence the rate constants, are identical within experimental error.

Table 1: Transient-State Determination of k_2 and k_3 at pH 5.0−10.5 using Ferulic Acid as Reducing Substrate

pH	k_2 (μM^{-1} s^{-1})	k_3 (μM^{-1} s^{-1})	k_2/k_3
5.0	8.5 ± 0.2	8.9 ± 0.3[a]	1
6.0	25.0 ± 1.2	22.2 ± 0.5[a]	1
7.0	≥63	41 ± 4[b]	1.5
8.0	≥120	48 ± 2[c]	3
8.5	≥97	44 ± 2[c]	2
9.0	≥73	18 ± 1[b]	4
9.5	≥63	8.7 ± 0.2[c]	7
10.0	38 ± 1	3.8 ± 0.05[c]	10
10.5[d]	18.8 ± 0.5	1.0 ± 0.02[c]	19

[a] Determined by direct measurement, method ib, at the isosbestic point between cpd I and II, in pH-jump experiments. [b] Determined both by the direct method (ia), and by the turnover method (ii), averaging the results. [c] Turnover method (ii) applied using both the isosbestic point between resting state CIP and cpd I and the isosbestic point between cpd I and II. Values shown as ≥ were too fast for accurate measurement. Fitting the data to equations with one or two pK_a values gave the same result for the alkaline transitions, pK_a 9.0 ± 0.7 for k_2 and 8.8 ± 0.4 for k_3. Acidic transitions are near 7. [d] pH-jump experiments.

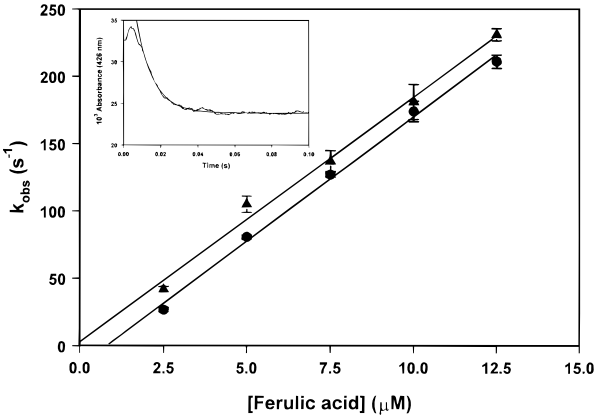

FIGURE 6: Determination of k_3 at pH 9.0 as the slope of k_{obs} vs concentration of ferulic acid using the direct method (i) (●) or the turnover experiment (inset), method (ii) (▲). In the inset, transient conversion of cpd I is observed before the reduction of cpd II. A fit of the latter reaction is shown.

The transient-state determinations of k_2 and k_3 are summarized in Table 1. It can be seen that k_2 and k_3 are of similar magnitude, as predicted from the steady-state experiments. The ratio k_2/k_3 increases with pH, from k_2 and k_3 being equal at low pH to k_2 10 times greater than k_3 at pH 10. An order-of-magnitude difference between k_2 and k_3 is normal for peroxidases (*31*).

The k_2 and k_3 rate constants were also estimated using ABTS as reductant. However, due to the large absorption of ABTS at the Soret maximum of CIP, the reactions were measured in the visible region (spectra from ref *30*). The value of k_2 was measured at 530 nm, an isosbestic point between cpd II and resting state CIP (Figure 7). k_3 was estimated using method (i) measuring at 576 nm, an isosbestic point between cpd I and cpd II. k_{obs} values could not be obtained over a range of ABTS concentrations, due to the limits set by the dead time of the instrument (2−3 ms), but only at a single concentration, 18.75 μM of ABTS and 3.5 μM of enzyme at pH 7.0. Despite the fact that 5-fold

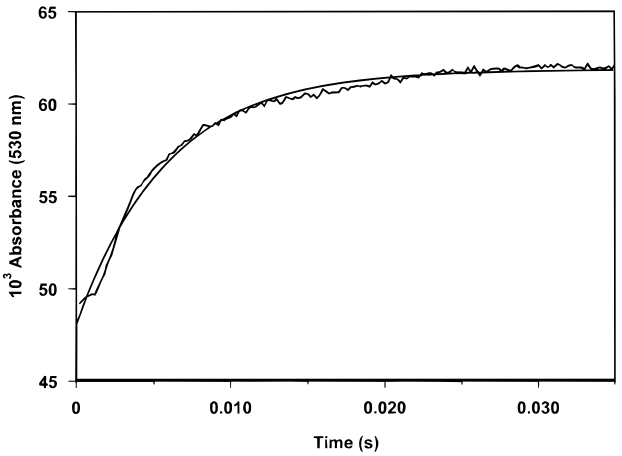

FIGURE 7: Transient-state determination of k_2 at pH 7 carried out in the visible region. Cpd I was reduced to cpd II by ABTS (see the text for details).

excess of substrate is at the limit of being pseudo-first-order, k_2 and k_3 were estimated assuming $k_{obs} = k$[ABTS]. The estimated values are $k_2 = (2.0 \pm 0.2) \times 10^7$ M^{-1} s^{-1} and $k_3 = (2.0 \pm 0.1) \times 10^7$ M^{-1} s^{-1}. The value of $k_2k_3/(k_2 + k_3)$, $(1.0 \pm 0.2) \times 10^7$ M^{-1} s^{-1}, calculated from the transient-state results is in reasonable agreement with the results of the steady-state experiments.

DISCUSSION

Structure of CIP. Yeast mitochondrial cytochrome *c* peroxidase CCP has been the most extensively studied peroxidase to date and has served as a model for the heme-site structure and reactions with H_2O_2 and small ligands. Crystallographic (*6*−*8*) and resonance Raman studies on CIP (*16*, *32*) show that CIP and CCP are similar at their heme sites. The proximal fifth ligand to the heme iron of CIP is His183, which is hydrogen-bonded to Asp245 (Figure 8A). In the distal cavity His55, hydrogen-bonded to Asn92, has a key role in the reaction with H_2O_2 and ligand-binding at the sixth site of coordination to heme iron. Also distal Arg51, hydrogen-bonded to the heme propionates via water molecules, is expected to have a minor role in these reactions as shown for CCP (*33*, *34*). CIP is more similar to horseradish peroxidase HRP C in all of its (eqs 1−3) in the peroxidase cycle and in its heme spin states and coordination at extremes of pH, but it is pure 5-coordinate high spin at neutral pH like CCP (*32*). In Figure 8A the heme-site structure of CIP at presumed physiological conditions is shown and provides a structural reference in which to explain the reaction between CIP and H_2O_2. The steady-state results, however, may also depend on the interaction site for aromatic substrates and products, which is thought to extend from the heme edge toward the entrance of the distal cavity. In CIP this site is very accessible compared to lignin peroxidase and is dominated by a number of glycine residues (Figure 8B) (*6*, *7*).

Rate of CIP Compound I Formation. Extensive spectral and transient-state kinetic analysis of CIP cpd I formation at 25 °C, pH 3.6−10.8, have been carried out previously (*30*). A pH-independent rate constant of $k_1 = (7.1 \pm 0.1) \times 10^6$ M^{-1} s^{-1} was found. In the present transient-state study at pH 7.0 $k_{1app} = (9.9 \pm 0.6) \times 10^6$ M^{-1} s^{-1}, confirming that the enzyme samples in the two studies are comparable. To further elucidate the mechanism of cpd I formation, comprehensive analyses are performed in the steady state using ABTS and ferulic acid as reducing substrates. At pH 7.0 and 25 °C, ABTS gave $k_1 = (6.7 \pm 0.2) \times 10^6$ M^{-1} s^{-1}, and ferulic acid $(8.8 \pm 0.6) \times 10^6$ M^{-1} s^{-1}, results similar to, but slightly lower than, those obtained in transient-state measurements. Previous but less detailed studies with the same conditions using guaiacol gave $(3.7 \pm 0.3) \times 10^6$ M^{-1} s^{-1} (*30*), and with ABTS and iodide $(7.9 \pm 0.2) \times 10^6$ M^{-1} s^{-1} and $(4.8 \pm 0.1) \times 10^6$ M^{-1} s^{-1}, respectively (*35*). The latter study also analyzed six CIP mutants with one or more bulky side chains at the heme pocket entrance, and found that k_1 for the mutants never decreased to less than half of the value for wild-type CIP in either assay.

The k_1 for CIP is near the average found for other heme-containing peroxidases. It is about 10- and 4-fold higher, respectively, than that for the structurally most similar fungal lignin and Mn peroxidases [lignin peroxidase, 4.2×10^5 M^{-1} s^{-1}, pH 3−6 (*36*), or 6.5×10^5 M^{-1} s^{-1} (*37*); Mn peroxidase, 2.0×10^6 M^{-1} s^{-1} (*38*)]. Horseradish peroxidases HRP C and A2 are 2-fold faster and 5-fold slower than CIP, respectively, 1.7×10^7 M^{-1} s^{-1} for HRP C (*39*) and 1.8×10^6 M^{-1} s^{-1} for HRP A2 (*40*). CCP is five-fold faster (4.6×10^7 M^{-1} s^{-1}) (*41*, *42*). Hence peroxidase cpd I formation is normally very fast, $k_1 \sim 10^7$ M^{-1} s^{-1}. Distal histidine is the essential catalytic residue and contributes by approximately 10^5 M^{-1} s^{-1} according to the results of mutational studies in CCP (*33*).

pH Dependence of CIP Cpd I Formation. The pH dependence of the steady-state reaction was examined over the pH range 3.8−10.0 (Figure 4) and gave a result similar to that obtained in the transient-state study. The rate of cpd I formation is unchanged up to pH 10.8, the highest pH examined. This is consistent with spectroscopic results (*24*, *32*), which show that the neutral five-coordinate high-spin form of CIP dominates and is still present in low amount at pH 12.1, where a six-coordinate low-spin OH^- form is found (*32*).

At acid pH the situation is unusual and more complex. Cpd I formation is linked to a transition with p$K_a = 5.1 \pm 0.1$, where the basic form is the more active. The transient-state study of k_1 uncovered the same pH dependence, giving p$K_a = 4.9 \pm 0.1$ (*30*), and cyanide binding to CIP decreased at low pH with p$K_a = 5.1 \pm 0.2$ (*25*). We have avoided the use of acetate and nitrate and have therefore not observed anionic effects previously noticed in HRP C and CCP studies (*39*, *43*). The crystal structure (*44*) and NMR analysis (*24*) of cyanide-bound CIP show that cyanide is hydrogen-bonded to distal histidine as in other known peroxidases. The kinetic data indicate, therefore, that the properties of distal His55 of CIP change dramatically at pH 5, due to either protonation or conformational change. These two possibilities will be considered in detail as CIP, in this respect, is very different from its fungal relatives lignin peroxidase and Mn peroxidase, both of which show k_1 rate constants that are independent of pH between values of 3−8 (*37*, *38*, *45*).

The active site of peroxidase is linked to a number of titratable groups: distal histidine, arginine, and water molecules, proximal histidine and aspartic acid, and the heme propionates (Figure 8A). The heme propionates are relatively exposed to solvent and might exhibit pK_as close to 5.5 and 4.5, values similar to those for dicarboxylic acids. However, cpd I formation is affected very little by their protonation state as shown by the kinetics of mono- and

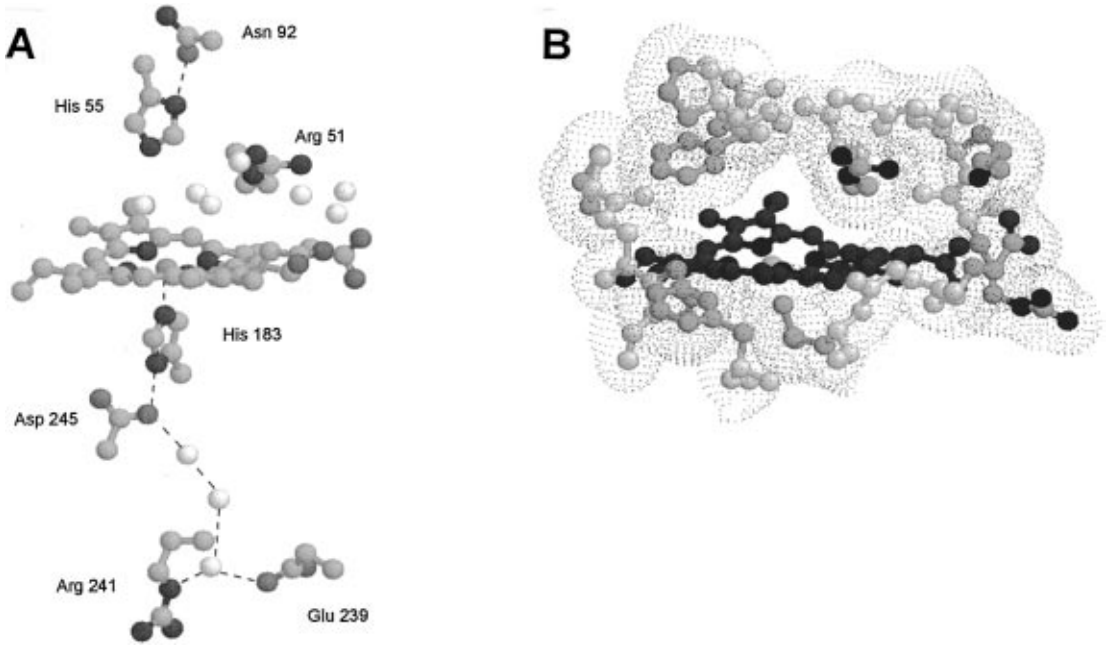

FIGURE 8: Heme active site of CIP. (A) Distal side chains of His55, Asn92, Arg51, and seven distal water molecules (white) are shown above the heme group, and the proximal His183, Asp245, three-water proton path to the molecular surface with Arg241 and Glu239 are shown below the heme. (B) Surface residues presumably involved in substrate binding and distal Arg51 and Phe54 are shown in van der Waals surface representation in the same orientation as panel A from the surface of the molecule along the hydrogen peroxide access channel toward the distal cavity (upper half). Nitrogen atoms are black; oxygen and heme are dark gray. The coordinates for ARP were kindly provided by Dr. K. Fukuyama (*8*), and the images were generated using the RasMol v2.6 visualization program by Dr. R. Sayle.

dimethyl propionate esters of HRP C (*46*) and of the dimethyl ester of CCP (*47*), and confirmed by pH-independent lignin and Mn peroxidase cpd I formation at pH 3−8. The principle of charge neutrality inside a protein will apply to the hydrogen-bonded proximal histidine−aspartic acid couple, linking their pK_a values. At neutral pH CIP has a strongly bound proton located at Asp245 (*15*, *32*), giving partial imidazolate character to proximal His183, as in other wild-type peroxidases. On the distal side, arginine will remain positively charged in the resting state over the entire pH range of peroxidase stability, including high pH values due to interaction with the negatively charged propionates and the OH^- ligand of heme iron, which is formed at pH > 11. The neutral form of histidine is favored in the interior of a protein (pK_a = 5.5 for distal histidine of methemoglobin), and in resting state peroxidase protonation will be further suppressed by the nearby positively charged distal arginine, predicting an abnormally low pK_a for distal histidine, that could well be outside the range of pH stability of peroxidase. The pK_a for HRP C cpd I formation is 2.5 in buffers excluding nitrate or acetate and is supposed to represent distal histidine. When the latter anions are present, the pK_a increases to 4.2 (*23*, *39*). A similar situation is found in CCP, where the pK_a is 4.0 in the absence of nitrate but 5.4 in its presence, i.e., similar to methemoglobin. There is evidence that nitrate interacts with distal arginine in CCP (*43*). The pK_a of distal histidine will be lower than 3 for both lignin and Mn peroxidase cpd I formation (see the previous paragraph) and has been estimated to be ≈1 for lignin peroxidase (*48*). pK_a values are very sensitive to the environment. Calculated electrostatic potentials of CIP, CCP, and lignin peroxidase (*49*) showed a significantly more positive potential at the active-site groups of CIP as compared to CCP and much more when compared to lignin peroxidase. The pK_a values of the active-site groups of CIP should be expected to be lower than for lignin peroxidase. We can therefore conclude that protonation of distal histidine is not the primary event linked with the pK_a of 5 for CIP cpd I formation.

Pronounced changes have been observed in CIP between pH 6.0 and 3.8 by electronic absorption and resonance Raman spectra (*30*, *32*), and magnetic circular dichroism also indicates a pK_a = 4.9 ± 0.1 (*50*). These spectral changes cannot be explained by protonation of a distal histidine residue but must involve the heme directly. Smulevich et al. (*32*) identified a new five-coordinate high-spin form with a Soret maximum at 394 nm that coexists with a very small amount of the normal five-coordinate high-spin form at pH 3.8, and they suggested that the proximal ligand bond to the heme iron had been severely weakened or broken as a result of protonation of proximal His183. NMR studies of resting state CIP pH 9.7−5.1 (*24*) showed very little change in the chemical shift values of the heme methyl resonances but some small shifts and intensity changes for the resonances of proximal His183 CβH$_2$ in the 30−50 ppm region going from pH 6.2 to 5.1. Due to solubility problems, these studies were not extended below pH 5.1. The spectroscopic and kinetic studies were performed in the same buffers and can therefore be related directly, whereas the crystal structure of CIP is unknown at 0.1 M ionic strength at low pH.[2] The acidic form of CIP is quite stable and presumably not dramatically different from the neutral active form (NMR data). We are therefore left with two questions: (i) Is it plausible that proximal His183 of CIP can be protonated with a pK_a of 5? (ii) Can the nature of the proximal ligand affect CIP cpd I formation and cyanide binding as observed?

[2] The crystal structure of CIP shown in Figure 8 (*8*) was determined by soaking a crystal in 50 mM sodium acetate buffer, pH 4.5, containing 35% (1.4 M) ammonium sulfate for 2 h. Like the authors, we consider this structure to represent the physiologically active form rather than the acidic inactive form, as a high concentration of ammonium sulfate will stabilize the more compact form and also affect pK_a values.

The first question can be answered in the affirmative. In CIP, the Asp245 oxygen, hydrogen-bonded to proximal His183, is at the same time hydrogen-bonded via a direct link of three water molecules to the molecular surface of CIP (*50*). The last water is hydrogen-bonded to the side chains of Glu239 and Arg241 (Figure 8A). This structural feature is conserved in fungal peroxidases. However, CIP differs from lignin and Mn peroxidases in three respects. First, the phenylalanine residue adjacent to proximal histidine in both lignin and Mn peroxidase is substituted to the smaller Leu200 in CIP, leaving more space for proximal rearrangement. Second, the heme group of CIP is much more exposed than in lignin and Mn peroxidases (Figure 8B). Third, Glu239 and the nearby Glu214 have been shown to destabilize CIP significantly due to electrostatic repulsion. Replacing Glu239 by neutral or basic residues stabilizes these CIP mutants greatly as compared to wild-type CIP (*51*). These three features, unique to CIP, may account for greater flexibility and ease of protonation of proximal His183 and Asp245 via the three-water path without pH denaturation of the whole molecule, and we propose that this is the primary event leading to the spectral changes linked with pK_a 5.0.

The second question cannot be answered definitively at the present. The substitution of proximal His175 of CCP by either glutamate or glutamine, which bind heme iron strongly and weakly, respectively (*52*), hardly affected cpd I formation (*53*). Substitution to glycine gave a bis-aquo-ligated CCP variant, which upon reaction with hydrogen peroxide gave Fe^{4+}═O; however, the rate was not reported (*54*). The heme had moved ≈0.5 Å in the direction of the propionates, and the overall activity was only 1.6% as compared with wt CCP. Therefore, it is still uncertain whether or not the nature of the proximal ligand (absent, water, or protonated) affects cpd I formation directly or rather only indirectly as a result of small geometric changes to the exact conformation and distances of distal histidine relative to heme iron. The coincident pK_a values for decrease in cpd I formation and cyanide binding to CIP are consistent with such an indirect effect following the protonation of His183.

Substrate Interaction. Steady-state analysis using ABTS at pH 7.0 reveals saturation kinetics (Figure 4), an unusual feature for peroxidases. The rate constant for the unimolecular step k_u is 1500 ± 100 s^{-1}. HRP C reacts similarly with ABTS giving a k_u value of 850 ± 40 s^{-1} at pH 7 (*29*). In agreement with the HRP C result we interpret k_u in terms of one or more rate-limiting dissociation steps of the ABTS radical from CIP cpd II or cpd I, although it could also represent other unimolecular steps. The binding of reducing substrates has been extensively studied by ^{1}H NMR spectroscopy based partly on the assumption that the cyanide-complexed peroxidase is a plausible model for either cpd I or II. The results obtained for HRP C showed interactions with the heme 8-methyl group and nearby protein side chains (*55*−*58*). These results were in agreement with the suicide inactivation experiments on HRP C and CIP (*59*, *60*), in which this heme site rather than the heme center was modified. The reduced labeling of the heme edge of CIP as compared to HRP C using various hydrazines was suggested by the authors to indicate a more buried heme in CIP. The crystal structure of CIP (Figure 8B) and the NMR identification of a number of phenylalanines and an isoleucine residue in the substrate binding site of HRP C show that this is not the case. On the contrary, product binding to CIP is generally even looser than to HRP C as observed here for ABTS; hence the time available for reaction at the heme edge. A weak binding of peroxidase radical products must be important in avoiding autooxidation or modification of the enzyme, thus increasing the turnover number. A similar conclusion was reached recently in a suicide inactivation study of HRP C mutants (*61*).

Structure and Reactions of Cpd I and Cpd II. Cpd I and II both contain Fe^{4+}═O and differ by only one electron on the porphyrin ring. Their structures are likely to be very similar as shown by X-ray absorption (*62*) and Mössbauer spectroscopic studies (*63*). The crystal structure of cpd I of CCP has been solved and shows that the N_ϵ of distal arginine and N_ϵ of distal tryptophan donate hydrogen bonds to ferryl oxygen (*64*, *65*). The fluoride complex of CCP shows the same pattern of hydrogen bonds (*66*). Likewise the presence of a hydrogen bond to ferryl oxygen in cpd II of HRP C at pH 7 but not at pH 10 has been suggested from X-ray absorption spectroscopic studies (*67*). We will assume that the cpd I and II structures of CIP and HRP C are very similar and that they differ from cpd I of CCP only by the substitution of distal tryptophan by phenylalanine. The OH^- and F^- complexes of CIP both show strong hydrogen bonding to positively charged distal arginine (*32*, *68*). Very recently, a simultaneous absorption and resonance Raman spectroscopy study of CIP (ARP) suggested that oxene of cpd I at pH 7.3 and of cpd II at pH 8.8 exchange with oxygen of the water solvent, whereas there is no exchange in cpd II at pH 10.7 (*69*). This could mean that the exchange is catalyzed by hydrogen bonding to arginine, and that distal arginine of CIP cpd II has a pK_a near 10, leading to disruption of the hydrogen bond. Kinetic evidence suggests that the one-electron reduction of the heme cation radical of cpd I is accompanied by the release of one proton from the substrate. The following one-electron reduction of the ferryl oxygen group of cpd II is also accompanied by the release of one proton (*23*). In addition, the ferryl oxygen must receive one or two protons and leave as hydroxyl or water, respectively, to complete the reaction cycle.

In the present kinetic study we have found that the k_2 and k_3 rate constants are of the same magnitude for ferulic acid and ABTS. Therefore $k_2k_3/(k_2 + k_3)$ and not k_3 was determined by steady-state measurements, giving (2.2 ± 0.1) × 10^7 M^{-1} s^{-1} for ferulic acid and (2.0 ± 0.7) × 10^7 M^{-1} s^{-1} for ABTS at pH 7.0. The high and similar k_2 and k_3 rate constants were determined by transient-state analyses, and their pH dependence was examined over the pH range from 5.0 to 10.5 using ferulic acid as substrate. From these data $k_2k_3/(k_2 + k_3)$ was calculated as 2.4 ×10^7 M^{-1} s^{-1} for ferulic acid at pH 7.0. A single confirmatory experiment at pH 7.0 was also carried out using ABTS, successfully monitoring the enzyme changes in the visible part of the absorption spectrum, and giving a calculated $k_2k_3/(k_2 + k_3)$ of 1.0 ×10^7 M^{-1} s^{-1}.

Cpd I was sufficiently stable in the whole pH range using a slight excess of hydrogen peroxide (*30*), whereas cpd II was obtained only at high pH in the same study and by Farhangrazi et al. (*70*). Here we obtained cpd II also at neutral pH by titrating cpd I with the slow substrate $K_4Fe(CN)_6$. Farhangrazi et al. (*70*) addressed the question of the unusual instability of cpd II of CIP compared to HRP C by measuring the reduction potentials of CIP cpds I and II from

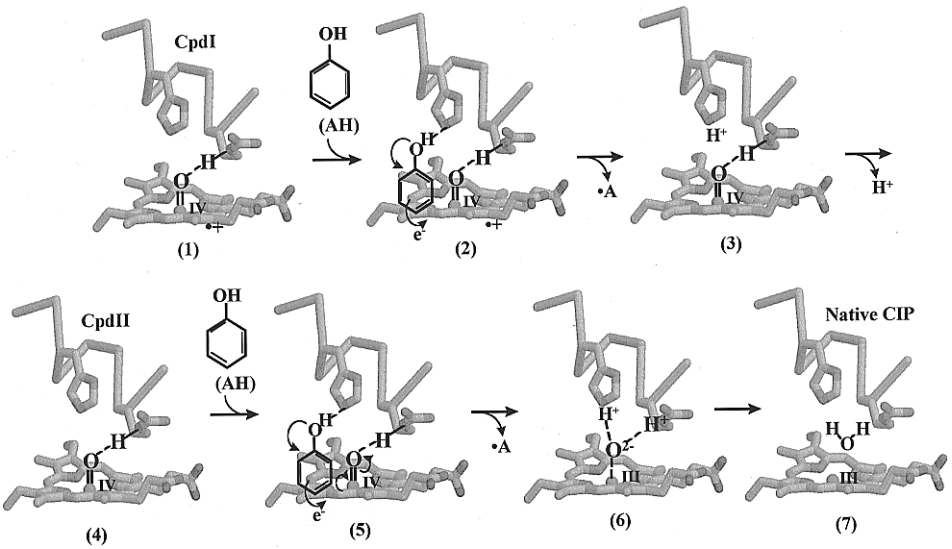

FIGURE 9: Proposed mechanism of cpd I and cpd II reduction in the catalytic cycle of CIP. The view is identical to that in Figure 8.

redox equilibria with hexachloroiridate at pH values from 6 to 9. Surprisingly, the reduction potentials were highest for cpd II, over the whole pH range. At pH 7 the values for CIP were 915 mV for cpd I and 982 mV for cpd II as compared to 880 and 900 mV for HRP C cpds I and II, respectively. The same authors found a k_2/k_3 ratio of about 3 at pH 7 using ascorbate as reducing substrate. Table 1 shows a k_2/k_3 ratio of 1 at low pH, whereas this ratio increases to 10 at pH 10. This pH-dependent change can be explained by a similar change of the ratio of the reduction potentials of cpd I and cpd II, as the latter decreases most at high pH. Hence we agree with Farhangrazi et al. (*70*) that the high k_3 values result from the unusually high reduction potential of CIP cpd II, but we disagree with their interpretation that cpd II of CIP is particularly unstable. At neutral pH and under steady-state conditions cpd II is highly reactive and not accumulated like cpd II of HRP C. The resulting technical problem of measuring k_3 was overcome by monitoring the reaction at a wavelength discriminating between cpd I and II.

Despite the fact that the reduction potentials of cpd I and II increase as the pH goes down, the rate constants show pK_a values near 7 (Table 1). Protonation of distal histidine is the most likely source, as the high electron density of ferryl oxygen may increase the pK_a for this residue in cpd I and II as compared to the resting state. The pK_as of ferulic acid are 4.4 and 9.0 (*28*) and therefore outside the range of the observed. If this is correct then distal His55 most likely assists in the catalytic removal of the protons from the reducing substrate, either through direct bonding or via intervening hydrogen-bonded water molecules. The first proton accepted during cpd I reduction is likely to be released to the solvent before the binding and reaction of the second substrate molecule to explain the similar pK_a of cpd II. The possibility of such a high pK_a for distal histidine is known for the cyanide-bound forms of HRP C (*71*) and CIP (*44*).

The rate constants k_2 and k_3 decrease at high pH values, partly as a result of the lower reduction potentials but also due to deprotonation reactions. pK_a values are observed at 9.0 ± 0.7 for k_2 and 8.8 ± 0.4 for k_3 (Table 1). The pK_a of 9.0 for the phenol to phenoxide ion transition of the ferulic acid seems the most plausible explanation in analogy with the reaction of HRP C cpd II and phenols, and in particular with *p*-methoxyphenol (*72*). This study concluded that the phenoxide ion was not a substrate. However, protonation of distal arginine of CIP cpd I and II expected near pH 10 (cf. resonance Raman results discussed above) cannot be distinguished unambiguously using only ferulic acid.

The reaction mechanism proposed for CIP cpd I and cpd II reactions is outlined in Figure 9. The scheme accommodates the kinetically derived ionizations observed, the findings of Ortiz de Montellano and co-workers (*59, 60*) that the reduction of cpd I of CIP and other peroxidases occurs at the heme edge, and the extensive structural information now available from X-ray crystallography and spectroscopic studies. The scheme implies that N_ϵ of distal arginine donates a hydrogen bond to ferryl oxygen in all intermediates and that the N_η nitrogens participate in extensive hydrogen bonding as observed for cpd I of CCP. In the final step the $N_\epsilon H$ could be donated as one of the protons to ferryl oxygen and arginine be reprotonated from the solvent via hydrogen-bonded water. Electron transfer from a substrate molecule AH to the porphyrin π-electron system proceeds via orbital overlap (reactions 1−2 and 4−5). Concurrently, unprotonated distal histidine, either directly or via hydrogen-bonded water, depending on the particular substrate, will abstract a proton from the substrate (reactions 1−2 and 4−5). The proton acquired in reaction 1−2 will be released to the solvent at the same time as the oxidized substrate A•. Distal histidine is assisted by its hydrogen-bonded network to the side chain of Asn92 which is further linked to the backbone carbonyl of Glu86, a feature conserved in CIP, CCP, and HRP C. The proton acquired in reaction 4−5 is readily available for the oxygen ligand of Fe at the same time as the ferryl is reduced to ferric by the electron abstracted from the second substrate molecule. In the final step the second A• will be released to the solvent, and the structure will relax to the resting state form of CIP.

Recent work on HRP C mutants actually ascribes a major role to the distal histidine network, not only in formation of cpd I but also in the reactions with reducing substrate. Changing asparagine in this network to valine effectively disrupts the network. The Asn70Val mutant of HRP C showed a 7-fold decrease in the k_2 value for cpd I reduction by guaiacol at pH 7.0 (*73*). It should be noted, however, that mutations in the distal histidine network most likely will

also affect the properties of the distal arginine, as the N_η atoms of this residue are hydrogen-bonded to the backbone carbonyls of the residue both before and after the network asparagine residue, at least in CCP and CIP (*44*).

Conclusions. In the present kinetic study of CIP (ARP), pH 5.0−10.5, we have elucidated the mechanism of action of resting state CIP with hydrogen peroxide and of the intermediates cpd I and II with a natural phenolic substrate, ferulic acid, and the analytical heterocyclic substrate ABTS. The results have been interpreted in structural terms on the basis of crystallographic, chemical modification, and NMR and resonance Raman spectroscopic information.

APPENDIX

Mechanism of peroxidase catalysis including slow product release:

$$E + H_2O_2 \xrightarrow{k_1} \text{cpd I} + H_2O \quad \text{(A1)}$$

$$\text{cpd I} + AH \xrightarrow{k_2} \text{cpd II} + A^\bullet \quad \text{(A2)}$$

$$\text{cpd II} + AH \xrightarrow{k_3} EA + H_2O \quad \text{(A3a)}$$

$$EA \xrightarrow{k_u} E + A^\bullet \quad \text{(A3b)}$$

Mass balance:

$$E_0 = [E] + [\text{cpd I}] + [\text{cpd II}] + [EA] \quad \text{(A4)}$$

$$\Updownarrow$$

$$[\text{cpd I}] = E_0/(1 + [E]/[\text{cpd I}] + [\text{cpd II}]/[\text{cpd I}] + [EA]/[\text{cpd I}]) \quad \text{(A5)}$$

Steady-state conditions:

$$d[E]/dt = k_u[EA] - k_1[E][H_2O_2] = 0 \quad \text{(A6)}$$

$$d[\text{cpd I}]/dt = k_1[E][H_2O_2] - k_2[\text{cpd I}][AH] = 0 \quad \text{(A7)}$$

$$d[\text{cpd II}]/dt = k_2[\text{cpd I}][AH] - k_3[\text{cpd II}][AH] = 0 \quad \text{(A8)}$$

$$d[EA]/dt = k_3[\text{cpd II}][AH] - k_u[EA] = 0 \quad \text{(A9)}$$

From steady-state and mass balance:

$$[\text{cpd I}] = E_0/\{1 + (k_2[AH])/(k_1[H_2O_2]) + k_2/k_3 + (k_2[AH])/k_u\} \quad \text{(A10)}$$

The initial rate:

$$v = -d[AH]/dt = k_2[\text{cpd I}][AH] + k_3[\text{cpd II}][AH] \quad \text{(A11)}$$

Combining eqs A8 and A11:

$$v = 2k_2[\text{cpd I}][AH] \quad \text{(A12)}$$

Combining eqs A10 and A12, and rearranging gives a standard format for the rate equation:

$$v/(2E_0) = A/(1 + B/[H_2O_2]) \quad \text{(A13)}$$

where

$$A = k_u/\{1 + [k_u(k_2 + k_3)]/(k_2k_3[AH])\} \quad \text{(A14)}$$

and

$$B = A/k_1 \quad \text{or} \quad k_1 = A/B \quad \text{(A15)}$$

Hence, parameter A plotted versus parameter B gives a straight line with the slope k_1, as for the classical peroxidase mechanism. It should also be noted that k_u is a true k_{cat} value for the modified reaction. This is unusual for peroxidases-for which it has generally been accepted that the second-order step cpd II reacting with reducing substrate is rate-limiting.

Using reducing substrates with no rate-limiting step (eq A3b), eq A14 is reduced to

$$A = [AH]k_2k_3/(k_2 + k_3) \quad \text{(A16a)}$$

If moreover, $k_2 \gg k_3$, which applies to most peroxidases, then

$$A = [AH]k_3 \quad \text{(A16b)}$$

REFERENCES

1. Welinder, K. G. (1992) *Curr. Opin. Struct. Biol. 2*, 388−393.
2. Shinmen, Y., Asami, S., Amachi, T., Shimizu, S., and Yamada, H. (1986) *Agric. Biol. Chem. 50*, 247−249.
3. Shinmen, Y., Asami, S., Amano, N., Amacho, T., Yoshizumi, H., and Kosugi, E. (1986) European Patent EP 0 104 074 B1.
4. Morita, Y., Yamashita, H., Mikami, B., Iwamoto, H., Aibara, S., Terada, M., and Minami, J. (1988) *J. Biochem. (Tokyo) 103*, 693−699.
5. Kjalke, M., Andersen, M. B, Schneider, P., Christensen, B., Schülein, M., and Welinder, K. G. (1992) *Biochim. Biophys. Acta 1120*, 248−256.
6. Petersen, J. W. F., Kadziola, A., and Larsen, S. (1994) *FEBS Lett. 339*, 291−296.
7. Kunishima, N., Fukuyama, K., and Matsubara, H. (1994) *J. Mol. Biol. 235*, 331−344.
8. Kunishima, N., Amada, F., Fukuyama, K., Kawamoto, M., Matsunaga, T., and Matsubara, H. (1996) *FEBS Lett. 378*, 291−294.
9. Baunsgaard, L., Dalbøge, H., Houen, G., Rasmussen, E. M., and Welinder, K. G. (1993) *Eur. J. Biochem. 213*, 605−611.
10. Baunsgaard, L., Vind, J., and Dalbøge, H. (1993) in *Plant Peroxidases*: *Biochemistry and Physiology* (Welinder, K. G., Rasmussen, S. K., Penel, C., and Greppin, H., Eds.) pp 239−242, University of Geneva, Switzerland.
11. Sawai-Hatanaka, H., Ashikari, T., Tanaka, Y., Asada, Y., Nakayama, T., Minakata, H., Kunishima, N., Fukuyama, K., Yamada, H., Shibano, Y., and Amachi, T. (1995) *Biosci. Biotech. Biochem. 59*, 1221−1228.
12. Dalbøge, H., Jensen, E. B., and Welinder, K. G. (1992) *Pat. Appl.* WO 92/16634.
13. Welinder, K. G., and Andersen, M. B. (1993) *Pat. Appl.* WO 93/24618.
14. Limongi, P., Kjalke, M., Vind, J., Tams, J. W., Johansson, T., and Welinder, K. G. (1995) *Eur. J. Biochem. 227*, 270−276.
15. Veitch, N. C., Tams, J. W., Vind, J., Dalbøge, H., and Welinder, K. G. (1994) *Eur. J. Biochem. 222*, 909−918.
16. Smulevich , G., Feis, A., Focardi, C., Tams, J., and Welinder, K. G. (1994) *Biochemistry 33*, 15425−15432.
17. Andersen, M. B., Johansson, T., Nyman, P. O., and Welinder, K. G. (1991) in *Biochemical Molecular and Physiological Aspects of Plant Peroxidases* (Lobarzewski, J., Greppin, H., Penel, C., and Gaspar, T., Eds.) pp 169−173, University of Geneva, Switzerland.
18. Akimoto, K., Shinmen, Y., Sumida, M., Asami, S., Amachi, T., Yoshizumi, H., Saeki, Y., Shimizu, S., and Yamada, H. (1990) *Anal. Biochem. 189*, 182−185.

19. Kim, B. B., Pisarev, V. V., and Egorov, A. (1991) *Anal. Biochem. 199*, 1−6.
20. Erman, J. E., and Vitello, L. B. (1993) in *Plant Peroxidases*: *Biochemistry and Physiology* (Welinder, K. G., Rasmussen, S. K., Penel, C., and Greppin, H., Eds.), pp 149−154, University of Geneva, Switzerland.
21. English, A. M., and Tsaprailis, G. (1995) *Adv. Inorg. Chem.* 43, 79−125.
22. Schuller, D. J., Ban, N., van Huystee, R. B., McPherson, A., and Poulos, T. L. (1996) *Structure 4*, 311−321.
23. Dunford, H. B. (1991) in *Peroxidases in Chemistry and Biology* (Everse, J., Everse, K. E., and Grisham, M. B., Eds.) Vol. 2, pp 1−24, CRC Press, Boca Raton, FL.
24. Veitch, N. C., Gao, Y., and Welinder, K. G. (1996) *Biochemistry 35*, 14370−14380.
25. Andersen, M. B., Hsuanyu, Y., Welinder, K. G., Schneider, P., and Dunford, H. B. (1991) *Acta Chem. Scand. 45*, 206−211.
26. Kulmacz, R. J. (1986) *Arch. Biochem. Biophys. 249*, 273−285.
27. Childs, R. E., and Bardsley, W. G. (1975) *Biochem. J. 145*, 93−103.
28. Rasmussen, C. B., Dunford, H. B., and Welinder, K. G. (1995) *Biochemistry 34*, 4022−4029.
29. Smith, A. T., Sanders, S. A., Thorneley, R. N. F., Burke, J. F., and Bray, R. C. (1992) *Eur. J. Biochem. 207*, 507−519.
30. Andersen, M. B., Hsuanyu, Y., Welinder, K. G., Schneider, P., and Dunford, H. B. (1991) *Acta Chem. Scand. 45*, 1080−1086.
31. Dunford, H. B., and Stillman, J. S. (1976) *Coord. Chem. Rev. 19*, 187−251.
32. Smulevich, G., Neri, F., Marzocchi, M. P., and Welinder, K. G. (1996) *Biochemistry 35*, 10576−10585.
33. Erman, J. E., Vitello, L. B., Miller, M. A., Shaw, A., Brown, K. A., and Kraut, J. (1993) *Biochemistry 32*, 9798−9806.
34. Miller, M. A., Shaw, A., and Kraut, J. (1994) *Struc. Biol. 1*, 524−531.
35. Tams, J. W., Vind, J., and Welinder, K. G. (1993) in *Plant Peroxidases: Biochemistry and Physiology* (Welinder, K. G., Rasmussen, S. K., Penel, C., and Greppin, H., Eds.) pp 143−148, University of Geneva, Switzerland.
36. Harvey, P. J., Palmer, J. M., Schoemaker, H. E., Dekker, H. L., and Wever, R. (1989) *Biochim. Biophys. Acta 994*, 59−63.
37. Marquez, L., Wariishi, H., Dunford, H. B., and Gold, M. H. (1988) *J. Biol. Chem. 263*, 10549−10552.
38. Wariishi, H., Dunford, H. B., MacDonald, I. D., and Gold, M. H. (1989) *J. Biol. Chem. 264*, 3335−3340.
39. Araiso, T., and Dunford, H. B. (1980) *Biochem. Biophys. Res. Commun. 94*, 1177−1182.
40. Kato, M., Aibara, S., Morita, Y., Nakatani, H., and Hiromi, K. (1984) *J. Biochem. (Tokyo) 95*, 861−870.
41. Loo, S., and Erman, J. E. (1975) *Biochemistry 14*, 3467−3470.
42. Vitello, L. B., Erman, J. E., Mauro, J. M., and Kraut, J. (1990) *Biochim. Biophys. Acta 1038*, 90−97.
43. Vitello, L. B., Erman, J. E., Miller, M. A., Wang, J., and Kraut, J. (1993) *Biochemistry 32*, 9807−9818.
44. Fukuyama, K., Kunishima, N., Amada, F., Kubota, T., and Matsubara, H. (1995) *J. Biol. Chem. 270*, 21884−21892.
45. Andrawis, A., Johnson, K. A., and Tien, M. (1988) *J. Biol. Chem. 263*, 1195−1198.
46. Araiso, T., Dunford, H. B., and Chang, C. (1979). *Biochem. Biophys. Res. Commun. 90*, 520−524.
47. Dowe, R. J., and Erman, J. E. (1982) *J. Biol. Chem. 257*, 2403−2405.
48. Cai, D., and Tien, M. (1991) *J. Biol. Chem. 266*, 14464−14469.
49. Welinder, K. G., Bjørnholm, B., and Dunford, H. B. (1995) *Biochem. Soc. Trans. 23*, 257−262.
50. Petersen, J. W. F. (1995) *Ph.D. Thesis*, University of Copenhagen, Denmark.
51. Cherry, J., Lamsa, M., Vind, J., Schneider, P., and Pedersen, A. (1995) in *Peroxidase Biotechnology and Application*, p 8 (abstr), Lomonosov Moscow State University, Russia, and University of Geneva, Switzerland.
52. Smulevich, G., Neri, F., Willemsen, O., Choudhury, K., Marzocchi, M. P., and Poulos, T. L. (1995) *Biochemistry 34*, 13485−13490.
53. Choudhury, K., Sundaramoorthy, M., Hickman, A., Yonetani, T., Woehl, E., Dunn, M. F., and Poulos, T. L. (1994) *J. Biol. Chem. 269*, 20239−20249.
54. McRee, D. E., Jensen, G. M., Fitzgerald, M. M., Siegel, H. A., and Goodin, D. B. (1994) *Proc. Natl. Acad. Sci. U.S.A. 91*, 12847−12851.
55. Veitch, N. C., and Williams, R. J. P. (1991) in *Biochemical, Molecular, and Physiological Aspects of Plant Peroxidases* (Lobarzewski, J., Greppin, H., Penel, C., and Gaspar, Th., Eds.) pp 99−111, University of Geneva, Switzerland.
56. La Mar, G. N., Hernández, G., and de Ropp, J. S. (1992) *Biochemistry 31*, 9158−9168.
57. Banci, L., Bertini, I., Bini, T., Tien, M., and Turano, P. (1993) *Biochemistry 32*, 5825−5831.
58. Veitch, N. C. (1995) *Biochem. Soc. Trans. 23*, 232−240.
59. DePillis, G. D., and Ortiz de Montellano, P. R. (1989) *Biochemistry 28*, 7947−7952.
60. Ortiz de Montellano, P. R. (1992) *Annu. Rev. Pharmacol. Toxicol. 32*, 89−107.
61. Gilfoyle, D. J., Rodriguez-Lopez, J. N., and Smith, A. T. (1996) *Eur. J. Biochem. 236*, 714−722.
62. Penner-Hahn, J. E., Eble, K. S., McMurry, T. J., Renner, M., Balch, A. L., Groves, T. J., Dawson J. H., and Hodgson, K. O. (1986) *J. Am. Chem. Soc. 108*, 7819−7825.
63. Schultz, C. E., Devaney, P. W., Winkler, H., Debrunner. P. G., Doan, N., Chiang, R., Rutter, R., and Hager, L. P. (1979) *FEBS Lett. 103*, 102−105.
64. Edwards, S. L., Xuong, N. N. H., Hamlin, R. C., and Kraut, J. (1987) *Biochemistry 26*, 1503−1511.
65. Fülöp, V., Phizackerley, R. P., Soltis, S. M., Clifton, I. J., Wakatsuki, S., Erman, J. E., Hajdu, J., and Edwards, S. L. (1994) *Structure 2*, 201−208.
66. Edwards, S. L., and Poulos, T. L. (1990) *J. Biol. Chem. 265*, 2588−2595.
67. Chang, C. S., Yamazaki, I., Sinclair, R., Khalid, S., and Powers, L. (1993) *Biochemistry 32*, 923−928.
68. Neri, F., Kok, D., Miller, M. A., and Smulevich, G., (1997) *Biochemistry 36*, 8947−8953.
69. Proshlyakov, D. A., Paeng, I. R., Paeng, K., and Kitagawa, T. (1996) *Biospectroscopy 2*, 317−329.
70. Farhangrazi, Z. S, Copeland, B. R., Nakayama, T., Amachi, T., Yamazaki, I., and Powers, L. S. (1994) *Biochemistry 33*, 5647−5652.
71. Thanabal,V., de Ropp, J. S., and La Mar, G. N. (1988) *J. Am. Chem. Soc. 110*, 3027−3035.
72. Dunford, H. B., and Adeniran, A. J. (1986) *Arch. Biochem. Biophys. 251*, 536−542.
73. Nagano, S., Tanaka, M., Watanabe, Y., and Morishima, I. (1995) *Biochem. Biophys. Res. Commun. 207*, 417−423.

BI970387R